Electronic Supporting Information

Influence of particle size on extraction from a charged bed – toward liquid marble formation

Casey A. Thomas[a], Moe Kasahara[b], Yuta Asaumi[b], Benjamin T. Lobel[a], Syuji Fujii[c,d], Peter M. Ireland[a], Grant B. Webber[a], Erica J. Wanless[a]

[a] Priority Research Centre for Advanced Particle Processing and Transport, University of Newcastle, Callaghan, NSW 2308, Australia

[b] Division of Applied Chemistry, Graduate School of Engineering, Osaka Institute of Technology, 5-16-1 Omiya, Asahi-ku, Osaka 535-8585, Japan

[c] Department of Applied Chemistry, Faculty of Engineering, Osaka Institute of Technology, 5-16-1 Omiya, Asahi-ku, Osaka 535-8585, Japan

[d] Nanomaterials Microdevices Research Center, Osaka Institute of Technology, 5-16-1 Omiya, Asahi-ku, Osaka 535-8585, Japan

Deposition of PPy-C_8F onto PS seed particles

The following protocol was used for coating the 20 μm-sized polystyrene (PS20) particles with a polypyrrole (PPy-C_8F) overlayer. Pyrrole (0.48 g, 4.0%) was added by syringe to a PS aqueous dispersion (144 g water and 12 g PS particles) in a 500 mL screw-capped bottle and the system was left for 3 h with magnetic stirring. C_8F aqueous solution (40 wt%, 2.98 g) was then added to the dispersion. $FeCl_3 \cdot 6H_2O$ oxidant (4.51 g) was dissolved in 96 g water and added to the aqueous dispersion of PS particles. The polymerisation was allowed to proceed for 24 h at 500 rpm using a magnetic stirrer. PPy-C_8F coating of the other PS seed particles with diameters of 40, 80 and 140 μm were also conducted by the chemical oxidative aqueous seeded polymerisation in the same manner, though the ratio of pyrrole monomer and the total surface area of the seed particles was adjusted to be the same as that of the 20 μm PS particle system see Table S1. The PPy-C_8F-coated PS particles were subsequently purified by repeated centrifugation-redispersion with sonication cycles (successive supernatants were replaced with de-ionised water) in order to remove the unwanted by-products (PPy-C_8F homopolymer, $FeCl_2$ and HCl), followed by freeze-drying overnight. PPy-C_8F bulk powder was synthesised by chemical oxidative precipitation polymerization as described in our previous study.[1] The nitrogen composition obtained by elemental analysis is also given in Table S1.

Table S1. Synthetic and particle characterisation data

Sample name	Pyrrole monomer concentration (wt%)	Nitrogen composition from elemental microanalysis (%)	Experimental PPy-C_8F loading, x (%)
PS20/PPy-C_8F	4.0	0.32	5.0
PS40/PPy-C_8F	2.0	0.07	1.1
PS80/PPy-C_8F	1.0	0.05	0.8
PS140/PPy-C_8F	0.6	0.05	0.8
PPy-C_8F	-	6.41	100

Polypyrrole shell layer thickness calculation

The shell layer thickness on each core-shell particle sample was calculated according to Eq. S1 below for which r_1 is the PS core radius (μm), r_2 is the PS/PPyC_8F core-shell radius (μm) as depicted in Fig. S1. x is the mass % of PPy-C_8F in the particle calculated by comparison to pure PPy-C_8F homopolymer in Table S1.

$$r_2 = \sqrt[3]{(r_1)^3 \times \left(1 + \frac{x}{100-x} \times \frac{\text{PS density}}{\text{PPy-C}_8\text{F density}}\right)} = \sqrt[3]{(r_1\ \mu m)^3 \times \left(1 + \frac{x}{100-x} \times \frac{1.060\times10^{-12}\ g/\mu m^3}{1.851\times10^{-12}\ g/\mu m^3}\right)} \quad \text{(S1)}$$

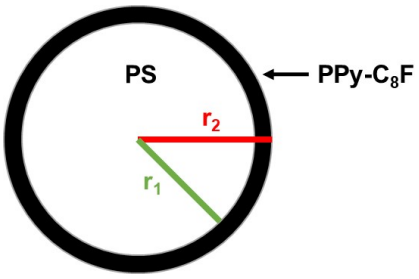

Figure. S1. Schematic for calculating the layer thickness of the PPy-C_8F coating on PS core particles.

Statistical model

As in Ireland et al. we use a weakest-link failure model, with the particle extraction probability given by a 3-parameter Weibull distribution.[3] This type of model is frequently used to predict failure in brittle solids, where an unknown but statistically quantifiable distribution of precursor flaws is present.[4] We assume that the probability of any specific particle in the area of interest being released from the bed can be given by:

$$P_{\mathrm{j}} = 1 - \exp\left[-\left(\frac{f_{\mathrm{z}} - f_{\mathrm{u}}}{f_0}\right)^m\right] \tag{S2}$$

f_{z} is the electrostatic extracting force in the normal direction per unit area of the top of the bed at the position of the single particle – i.e. the electrostatic pressure. This plays the same role as the tensile stress in fracture models. f_{u} is the minimum electrostatic pressure at which a particle will be extracted. f_0 is a characteristic value giving the scale of the distribution; namely, the value of $f_{\mathrm{z}} - f_{\mathrm{u}}$ at which the probability of extraction of a randomly-selected particle is $1 - e^{-1}$. The index m affects the spread of electrostatic pressures at which particle extraction occurs, a higher value indicating a narrower spread of pressures. f_{u}, f_0 and m are all characteristics of the bed, independent of the electric field. The effects of particle size, cohesiveness, etc. are all incorporated into these parameters.

The probability that a given particle *cannot* be extracted is the complement of P_{j}, i.e.

$$1 - P_{\mathrm{j}} = \exp\left[-\left(\frac{f_{\mathrm{z}} - f_{\mathrm{u}}}{f_0}\right)^m\right] \tag{S3}$$

For an area containing N identical particles, subjected to a uniform electrostatic pressure, the probability that *none* of them will be extracted is given by

$$1 - P_{\mathrm{j}}^{\text{ensemble}} = \left(1 - P_{\mathrm{j}}\right)^N \tag{S4}$$

Thus, for an area A with ρ particles per square metre (i.e. N = ρA), we can rearrange Eq. S2 to obtain the probability that *at least one* particle will be extracted, P_0:

$$P_0 = 1 - \exp\left[-\rho A\left(\frac{f_{\mathrm{z}} - f_{\mathrm{u}}}{f_0}\right)^m\right] \tag{S5}$$

If the electrostatic pressure is non-uniform on the area of interest, Eq. S4 must be integrated over the affected area of the top of the bed. For a radially-symmetric field, as in this case, this is:

$$P_0 = 1 - \exp\left[-2\pi\rho\int_0^{r_{\max}}\left(\frac{f_{\mathrm{z}} - f_{\mathrm{u}}}{f_0}\right)^m r\, dr\right] \tag{S6}$$

where r is the radial distance from the axis of the system and $r_{\max}$ marks the outer edge of the area of interest. The electric field is approximated by that between a conducting plane and sphere, using the model of Morrison (1989).[1] Since the bed is assumed to be conducting, the electric field at its surface is assumed to be entirely normal to the surface. The electrostatic normal pressure will be given in terms of the normal electric field, E_{z}, by

$$f_{\mathrm{z}}(r) = \sigma(r)E_{\mathrm{z}}(r) \tag{S7}$$

where σ is the charge per unit area of the top of the bed. By Gauss's Law,

$$\sigma(r) = \varepsilon_0 E_z(r) \tag{S8}$$

where ε_0 is the permittivity of free space, and thus

$$f_z(r) = \varepsilon_0 E_z(r)^2 \tag{S9}$$

According to the field model,

$$f_z(r) = \frac{\varepsilon_0 V^2}{a^2} \times H(\alpha, \delta) \tag{S10}$$

where V is the driving voltage, a is the sphere (drop) radius, $\alpha = r/a$ is the dimensionless radial coordinate and $\delta = h/a$ is the dimensionless sphere-plane separation. H is thus a function that gives the distribution of the electrostatic pressure in terms of the dimensionless geometry of the system. If we let H_u be the minimum extraction pressure, f_u, made dimensionless by the same scaling as in Eq. S10, we can now write

$$P_0 = 1 - \exp\left[-2\pi\rho a^2 \left(\frac{\varepsilon_0 V^2}{f_0 a^2}\right)^m \int_0^{\alpha_{max}} [H(\alpha, \delta) - H_u]^m \alpha \, d\alpha\right] \tag{S11}$$

The integral in Eq. S11 cannot be evaluated analytically, and must be determined numerically for m, H_u and δ. This was done for a set of over 4000 points covering the entire relevant range of these parameters, and invertible interpolation functions found. We denote these functions corporately as

$$G(\delta, m, H_u) \cong \int_0^{\alpha_{max}} [H(\alpha, \delta) - H_u]^m \alpha \, d\alpha \tag{S12}$$

and thus:

$$G(\delta, m, H_u) \cong -\frac{1}{2\pi\rho a^2}\left(\frac{f_0 a^2}{\varepsilon_0 V^2}\right)^m \ln(1 - P_{FPJ}) \tag{S13}$$

allowing us to determine the height at which the first particle is extracted from the bed, h_0, as a function of the probability, P_0:

$$\frac{h_0}{a} = \delta_0 \cong G^{-1}{}_{[m,H_u]}\left[-\frac{1}{2\pi\rho a^2}\left(\frac{f_0 a^2}{\varepsilon_0 V^2}\right)^m \ln(1 - P_0)\right] \tag{S14}$$

where $G^{-1}{}_{[m,H_u]}$ indicates inversion with respect to δ only (i.e. for given values of m and H_u). It is now possible to determine the envelope of separations where the first particle is observed to be extracted from the bed for a given driving voltage and probability range (e.g., 5% to 95%) and compare these to drop-bed separation data. It is worth noting that ρ and f_0, if both unknown, are not individually distinguished by the model; we therefore let

$$K = \frac{2\pi\rho}{f_0^m} \tag{S15}$$

and thus

$$h_0 \cong a G^{-1}{}_{[m,H_u]}\left[-\frac{1}{K}\frac{a^{2m-2}}{\varepsilon_0{}^m V^{2m}} \ln(1 - P_0)\right] \tag{S16}$$

It remains to determine which values of m, K and F_u are most consistent with a set of voltage-bed separation data. For each experimental data point i, Eq. S6 is used to calculate the significance (i.e. the theoretical probability of occurrence) of the measured drop-bed separation for V, and for proposed values of m, K and f_u. This significance measure is denoted S_i. If the model is correct, a plot of cumulative frequency vs. significance for a large number of data points, N, will be a straight line through the origin with slope N. Thus, a least-squares linear regression analysis is performed between the set of cumulative frequency vs. S_i data, and this 'ideal' cumulative frequency distribution.

Comparison of PS40 and PS80 data for drop-bed separation

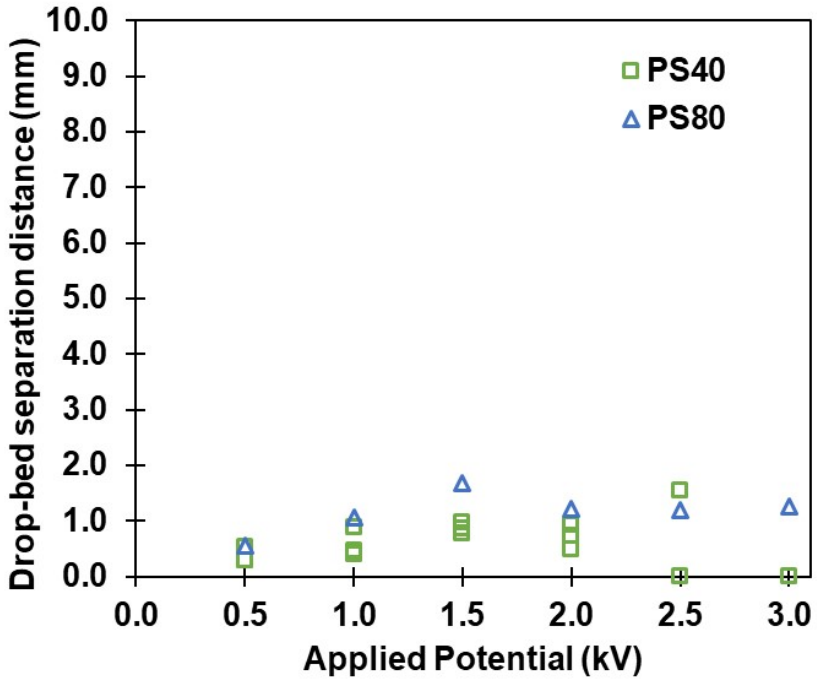

Figure S2. Measured drop-bed separation distance when uncoated particles are first observed to be extracted from the bed, as a function of applied potential. Both PS particle samples are used as received from supplier. At higher potentials, PS40 particles are not observed to be extracted from the bed, due to increased cohesion. All data points shown here sit below those of the samples shown in the main text, due to decreased conductivity and therefore an increased difficulty in extraction.[6]

References

1. H. Kawashima, H. Mayama, Y. Nakamura and S. Fujii, Polymer Chemistry, 2017.
2. P. M. Ireland, C. A. Thomas, B. T. Lobel, G. B. Webber, S. Fujii and E. J. Wanless, Journal of Physics: Conference Series, 2019, *in press*.
3. W. Weibull, Journal of Applied Mechanics, 1951, 18, 293-297.
4. R. F. Cook and F. W. DelRio, Experimental Mechanics, 2019, 59, 279-293.
5. C. A. Morrison, The potential and electric fields of a conducting sphere in the presence of a charged conducting plane, Adelphi MD: Harry Diamond Labs 1989.
6. C. A. Thomas, K. Kido, H. Kawashima, S. Fujii, P. M. Ireland, G. B. Webber, E. J. Wanless, Journal of Colloid and Interface Science, 2018, 529, 486-495.